Paper AAS 01-410

MARS GLOBAL SURVEYOR: MAPPING ORBIT EVOLUTION AND CONTROL THROUGHOUT ONE MARS YEAR

Pasquale Esposito, Eric Graat, Stuart Demcak*, Darren Baird and Vijay Alwar

Jet Propulsion Laboratory
California Institute of Technology
Pasadena, California 91109-8099

***OAO Corporation, Altadena, CA**

AAS/AIAA Astrodynamics Specialists Conference

Quebec City, Quebec, Canada July 30-August 2, 2001

AAS Publications Office, P.O. Box 28130, San Diego, CA 92198

AAS 01-410

MARS GLOBAL SURVEYOR: MAPPING ORBIT EVOLUTION AND CONTROL THROUGHOUT ONE MARS YEAR

Pasquale Esposito, Eric Graat, Stuart Demcak*, Darren Baird, Vijay Alwar

Jet Propulsion Laboratory, California Institute of Technology
4800 Oak Grove Drive
Pasadena, CA 91109-8099
* OAO Corporation, Altadena, CA

This paper presents the evolution and control of Mars Global Surveyor's (MGS) mapping orbit throughout one Mars year of the primary mapping mission. Starting on 3/9/99, after the completion of the second phase of aerobraking, this phase had a duration of 695 days or 8,505 orbits and ended on 2/1/01. At present, the project is in an extended mission which shall end on 4/22/02. The MGS orbit is the first short period, low altitude, nearly circular and polar, frozen-orbit and sun-synchronous orbiter of Mars.

The two major effects influencing the orbit evolution are a) small, frequent and nearly instantaneous velocity perturbations induced by the spacecraft's angular momentum desaturations (AMD) and b) the gravity field of Mars. The accumulated effect of AMDs has had a significant effect on the semi-major axis and, therefore, on the ground track walk and the uniform distribution of the ground tracks. In addition, predicting the influence of AMDs directly impacts the accuracy of the predicted time of descending equator crossings,Tdeqx, which is necessary for precise image targeting.

Current plans for MGS are: a) continue science observations at least until 4/22/02, b) assist Mars Odyssey during aerobraking as an early warning system for the detection of dust storms, c) obtain high resolution images of potential landing sites for the Mars Exploration Rover Mission (MER) and d) to act as a relay satellite for telemetry transmission during the descent phase of the two MER rovers.

INTRODUCTION

The purpose of this paper is to: a) present the Mars Global Surveyor (MGS) orbit element evolution of this unique mapping orbit throughout one Mars year (687 earth days), b) tabulate orbit controlling, propulsive maneuvers executed during this period, c) investigate orbital perturbations due to discrete and frequent spacecraft thrusting, on average every 7.5 hours, in order to desaturate angular momentum accumulated in three reaction wheel assemblies (RWA) and d) assess the accuracy of predicted time of equator

crossings, Tdeqx, over a 180 day interval. The accuracy of these predictions have a major dependency on the orbital effect of future, autonomous AMDs. In addition, this prediction is complicated by thruster plume impingement on the high gain antenna (HGA) in the environment of a variable HGA attitude profile during an orbit.

MGS's mapping phase began on 3/9/99 and ended 695 days later on 2/1/01 which encompassed a little more than one Mars year. The design of this unique mapping orbit (Ref. 1), that is, short period, low altitude, nearly circular, nearly polar, frozen, sun-synchronous and with a seven sol (one sol equals one Mars day) near repeat orbit cycle, was optimized to achieve the science objectives of the five MGS instruments (Ref. 2). At present, MGS is in an extended mission phase whose duration is from 2/1/01 to 4/22/02. Planning is in progress to utilize MGS as a relay satellite for the entry, descent and landing (EDL) phase of the two Mars exploration rovers (MER) scheduled to land on 1/4/04 and 1/25/04.

EVOLUTION OF THE MAPPING ORBIT PARAMETERS

Ground Track Walk (GTW) and Distribution

From a science perspective, the evolution of the ground track walk and the resulting distribution of ground tracks is of major importance for uniform and complete Mars data acquisition. MGS science data acquisition is continuous and acquired from a nadir pointing spacecraft which is maintained by a Mars horizon sensor. Thus, a non-uniform ground track distribution causes gaps in science observations especially if an instrument has a small field-of-view. Ideally, the mapping orbit design called for a constant GTW of 58.6 km eastward after a cycle of eighty-eight orbits or seven sols. The GTW, in km, is defined as

$$\text{GTW, km} = [\ \lambda(n) - \lambda(n-88)\ ]\ 3393.4\ (\pi/180) \qquad (1)$$

where $\lambda(n)$ is the longitude of the descending equator crossing (DEQX) at orbit n and eighty-eight orbits earlier and 3393.4 km is the mean Mars equatorial radius used in flight operations. If the GTW was constant at 58.6 km eastward throughout the mapping mission then uniform ground tracks would have been achieved with a 3 km spacing at the equator. Furthermore, the uniform 3 km spacing distribution would have been achieved over a supercycle of 6917 orbits or 550 sols. This was the goal of the MGS mapping orbit. The actual or achieved GTW evolution over the primary mapping mission and five months into the extended mission is shown in Figure 1. Initially, that is, after the transfer to the mapping orbit maneuver (Ref. 3) and the start of mapping, the GTW was 27.8 km. Orbit trim maneuvers, OTM-1 and OTM-2, achieved a "more frozen" mapping orbit and corrected the GTW as shown. Because of the GTW drift, OTM-3 further refined the GTW as indicated in Figure 1. After this, the GTW remained reasonably constant near the ideal value until solar conjunction on 7/1/00. During this time the perturbing influence of the AMDs changed dramatically causing a steep, negative trend in the GTW.

Major mission events, pertinent to navigation, are given in this figure and summarized in Table 1.

We now examine the influence of the GTW variation on the distribution of ground tracks over the primary mission. All orbit longitudes at AEQXs, that is, ascending or day side equator crossings, were compiled and ordered smallest to largest. Next sequential longitude differences were formed, $\Delta\lambda(n) = \lambda(n)-\lambda(n-1)$ and a frequency diagram of these differences was generated. Since $\Delta\lambda(max)=0.3$ deg (=18 km at the equator), 24 bins were created with 0.0125 deg = 0.375 km intervals. The results are shown in Figure 2 with the following conclusions: a) there are no longitude separations greater than 0.3 deg so the upper limit for ground track gaps at the equator is 18 km, b) 95.7% and 48.7% of the longitude separations are less than 0.15 deg (=9.0 km) and 0.025 deg (=1.5 km) respectively, and c) 34.6% of the longitude separations are in the 0.025-0.075 deg (1.5-4.5 km) range. In principle, if the GTW had been close to the ideal value throughout the primary mission then almost all the longitude separations would have been in the 0.025-0.075 deg range. Note that we have only considered AEQXs because they apply to the Mars Orbiter Camera (MOC); other instruments can acquire data throughout the entire orbit and thus there are twice as many equator crossings.

Table 1

MAPPING PHASE MAJOR MISSION EVENTS

Event	Date	Comment
Start mapping mission	03/09/99	DEQX orbit convention
Deploy HGA (orbit 247)	03/29/99	Frequent attitude control thrusting
MGS in contingency mode	04/16/99	HGA azimuth gimbal restriction
OTM-1 (orbit 729)	05/07/99	ΔV = 3.54 m/s
OTM-2 (orbit 1144)	06/10/99	ΔV = 0.18 m/s
OTM-3 (orbit 1905)	08/11/99	ΔV = 0.37 m/s
Start beta supplement	02/07/00	Earth beta angle = 43 deg
Mars superior conjunction	07/01/00	Restricted commanding
Edge-on orbit	12/15/00	Earth beta angle is zero deg
X RWA failure (orbit 8342)	01/18/01	Switch to S RWA
Start extended mission	02/01/01	Orbit 8505 (694.9 days)
Edge-on orbit	03/03/01	Earth beta angle is zero deg
Start AEM AMD (orbit 9193)	03/29/01	Reduce fuel usage
MGS in contingency mode	05/02/01	Sun ephemeris monitor error
End beta supplement	06/20/01	Earth beta angle = 43 deg
End surface occultations	07/23/01	Earth beta angle = 64.1 deg
Near face-on orbit	09/22/01	Earth beta angle = 79.0 deg
Begin surface occultations	12/03/01	Earth beta angle = 62.8 deg
Start beta supplement	03/17/02	Earth beta angle = 43 deg
End extended mission	04/22/02	

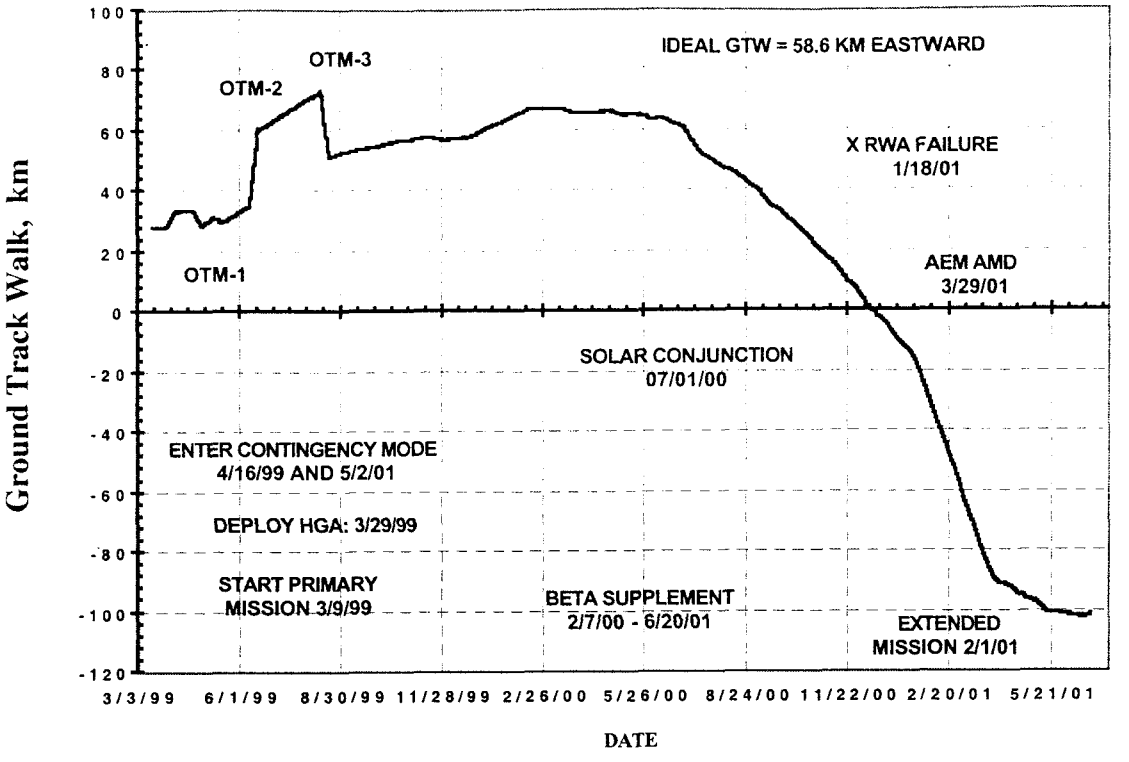

Figure 1 MGS Ground Track Walk From 3/9/99 To 6/25/01

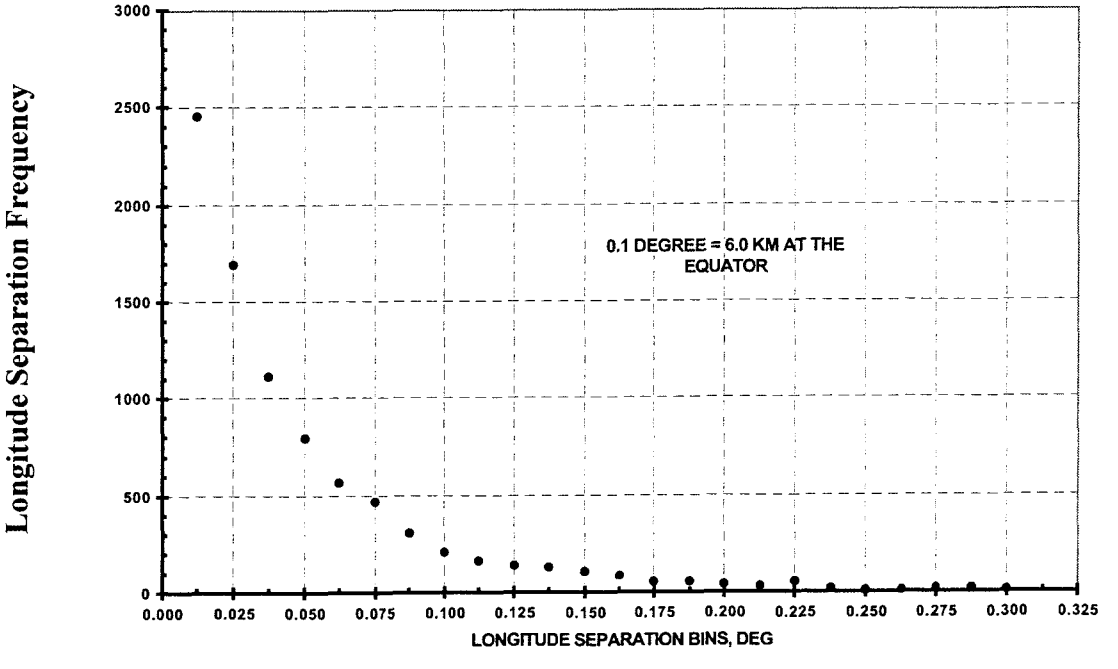

Figure 2 Distribution Of MGS Ground Tracks At AEQXs, Orbits 1-8506

The earth beta angle is equivalent to the angle between the MGS orbit plane and the direction from Mars to earth. An earth beta angle of zero degrees corresponds to an edge-on orbital configuration as seen from earth. On 4/15/99, a spacecraft anomaly developed whereby the azimuthal motion of the HGA was restricted apparently by a physical obstruction. Thus, the HGA could not follow the planned range of motion necessary to communicate with earth from early February 2000 to mid-June 2001 when the earth beta angle was below 41.5 degrees. This problem was solved by developing a new plan to operate the HGA in a previously unused range of earth beta or spacecraft azimuth angles which are the supplement of those in the nominal operating plan. This new mode of flight operations was called beta supplement and lasted from 2/7/00 to 6/20/01 (Ref. 4).

Frozen MGS Orbit and Altitude Variation

The concept of the "frozen orbit" refers to balancing the Mars gravity field perturbations between the orbital eccentricity and argument of periapsis such that the orbit's shape and apsidal rotation remain nearly constant in time (Refs. 1 and 5). This in turn leads to smaller orbital altitude variation than would have otherwise been possible by passive means. The time history of the osculating eccentricity (e) and argument of periapsis (ω), evaluated at apoapsis passage, is given in Figures 3 and 4 respectively. Clearly shown is the effect of OTM-1, to reduce the variation in both e and ω, and OTM-3 to center ω at 270 degrees true anomaly. After the three OTMs were executed, ω had a mean value of 270 deg with a 4 deg peak-to-peak variation and the eccentricity variation was less then 0.001. The failure of the X-axis RWA on 1/18/01 and its replacement by the S (skew) RWA resulted in a new AMD-induced perturbation with the orbital effects shown in these figures. Both these figures have been combined, although over a reduced time span from 3/9/99 to 8/11/99, to emphasize the e-ω variation before and after the OTMs and the refinement of the frozen orbit (Figure 5). Finally, the altitude variation at periapsis and apoapsis passage, with respect to a Mars reference surface defined by a mean equatorial radius of 3393.4 km and a flattening of 0.0052083, is given in Figures 6 and 7. The increasing altitude trend, especially evident after solar conjunction, may influence the decision to perform a planetary protection maneuver currently scheduled at the end of the mission. Note that there are short-term periodic and quasi-periodic variations with periods of 12-24 hours embedded in these long-term trends.

Local Mean Solar Time (LMST) and Orbit Inclination Variation

Originally, the MGS mapping orbit was designed to be sun-synchronous at 2:00 pm local mean solar time (LMST) at the DEQX in order to achieve constant lighting conditions for the science instruments. However, because of the –X axis solar array deployment problem experienced on launch day (11/7/96) and the extent of solar array-yoke degradation experienced early during aerobraking (10/11/97, Ref. 6), a redesign of the aerobraking strategy was necessary. This resulted in a modified mapping orbit with sun synchronism at 2:00 am LMST at the DEQX. With the successful conclusion of aerobraking on 2/19/99, the mapping mission began on 3/9/99 with orbit parameters given in Table 2.

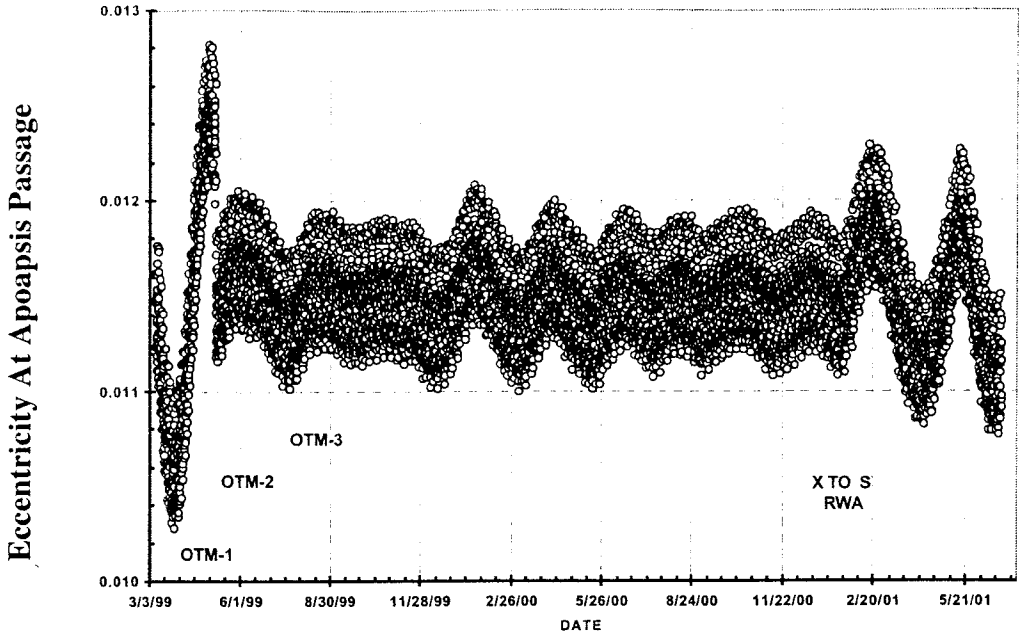

Figure 3 Osculating Eccentricity Variation (3/9/99 To 6/25/01)

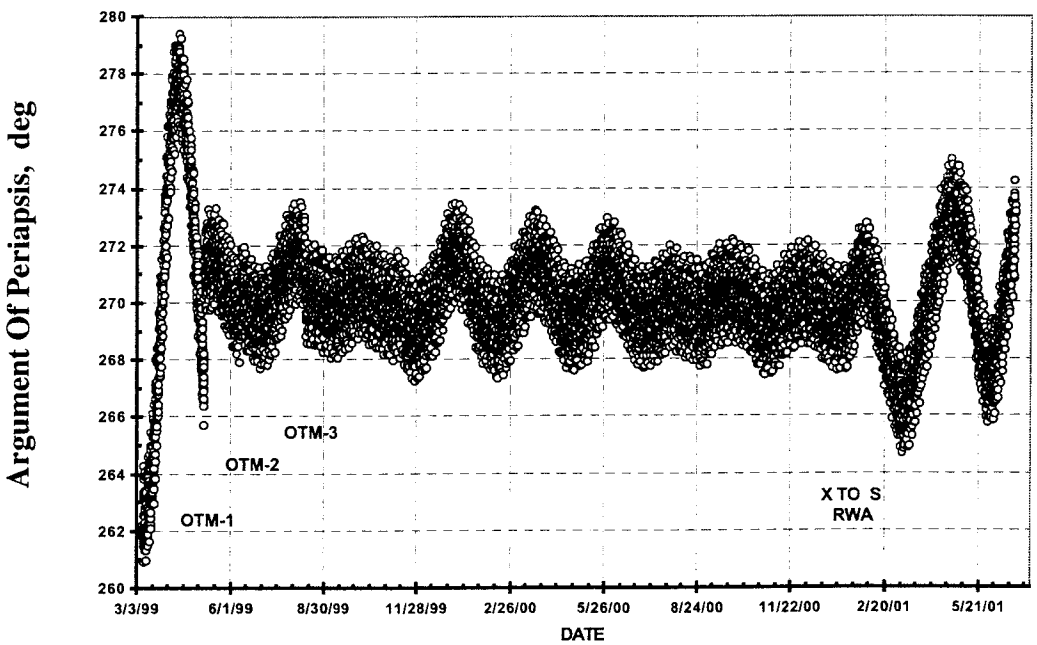

Figure 4 Argument Of Periapsis Variation (3/9/99 To 6/25/01)

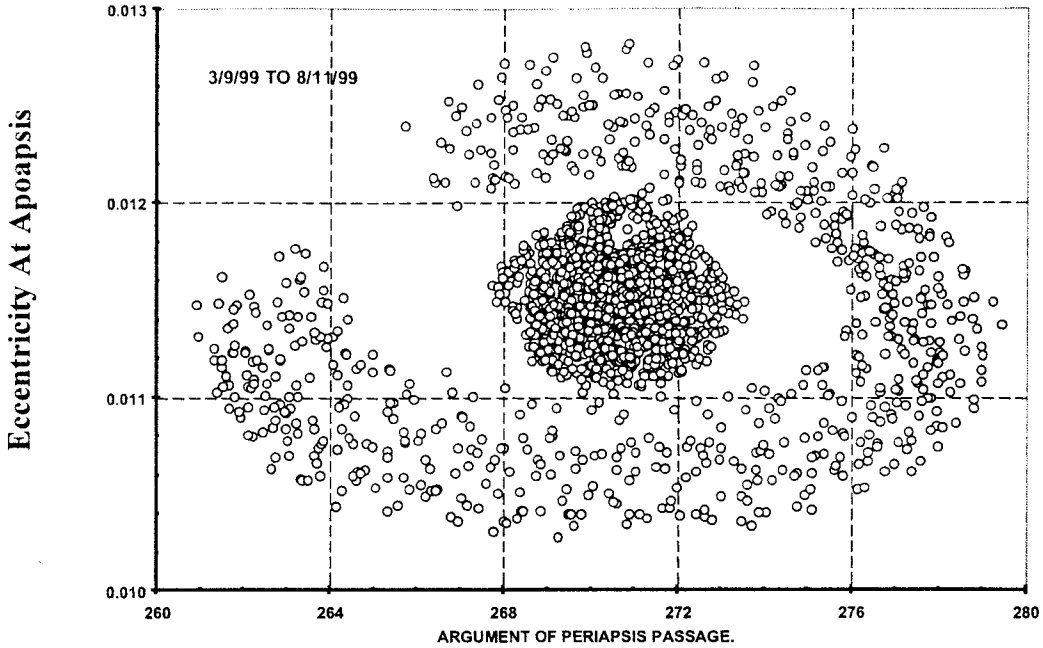

Figure 5 Phase Diagram Of Frozen Orbit (3/9/99 To 8/11/99)

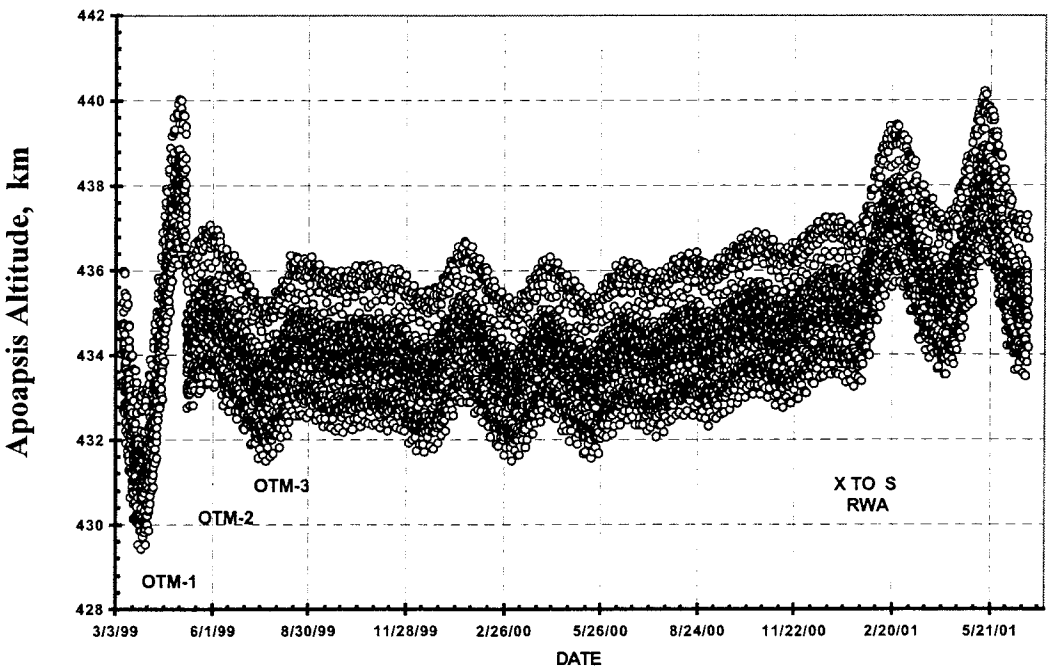

Figure 6 Altitude Variation at Apoapsis Passage (3/9/99 To 6/25/01)

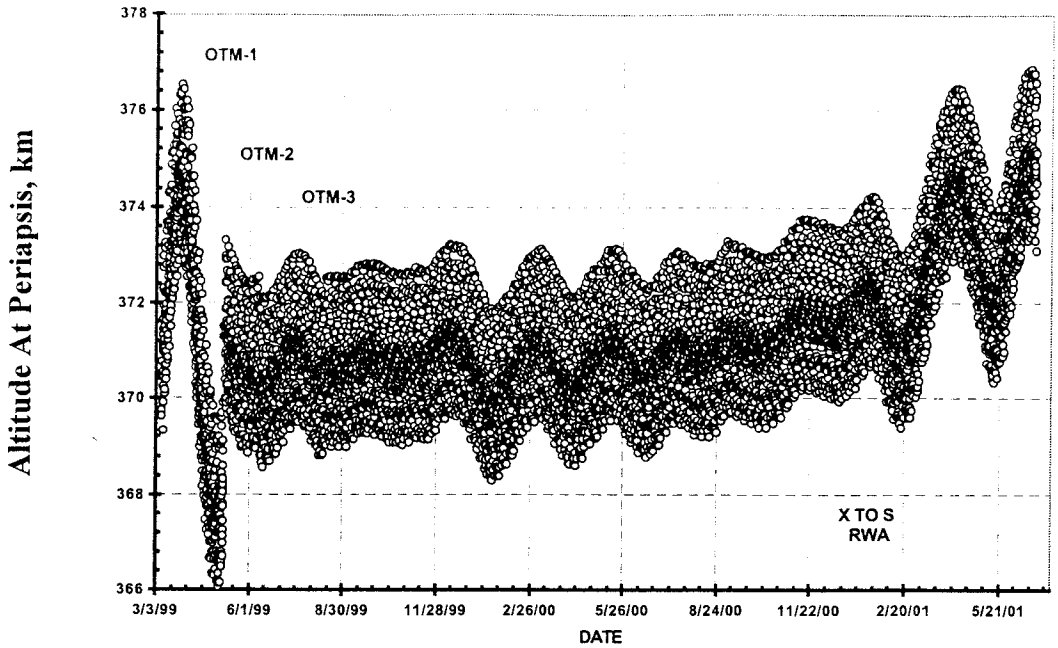

Figure 7 Altitude Variation At Periapsis Passage (3/9/99 To 6/25/01)

The coordinate system is Mars centered, Mars mean equator of date and earth mean equator of epoch J2000. Note that for the first twenty days of mapping, the HGA was in a fixed or undeployed position; HGA deployment was successfully achieved on 3/29/99. The variation in the LMST throughout the mapping phase is given in Figure 8; this is within the requirement of ten minutes of tolerance centered on 2:00 am. Closely related to the LMST is the inclination variation which is shown in Figure 9. Over the primary mapping mission, there is a secular increase in inclination of approximately 0.02 degrees. Monitoring this trend is important because of its potential impact on the nodal rate and ultimately on the sun-synchronism. The mean nodal rate achieved throughout mapping is 0.5237 degrees per day which differs slightly from the motion of the fictitious mean sun of 0.5240 degrees per day. The three minor breaks in the pattern shown in this figure are due to orbit determination degradation experienced at these times. The first refers to solar conjunction (7/1/00) when Doppler data were both sparse and noisy. The degradation at the remaining times (12/15/00 and 3/3/01) is due to an edge-on orbital configuration as seen from earth. During this configuration, orbit orientation angles especially the inclination, are more difficult to determine and thus have larger uncertainty.

Table 2
MGS ORBIT ELEMENTS DURING THE MAPPING PHASE

Element	Periapsis 1	Periapsis 4253	Periapsis 8505
Semi-major axis, km	3767.096	3765.622	3767.690
Eccentricity	0.00548	0.004995	0.005551
Inclination, deg	92.908	93.001	92.971
Arg of periapsis, deg	264.878	269.451	269.403
Long of ascend node, deg	7.971	189.526	11.775
Epoch, ET	03/09/99	02/19/00	01/31/01
Epoch, hr:min:sec	02:41:35	12:23:00	22:54:56
Period, seconds	7019.8	7015.7	7021.5
Altitude, km	370.533	371.035	370.999
LMST at DEQX, h:m:s	02:02:46	02:00:45	02:01:30
Nodal period, seconds	7060.2	7055.8	7062.7

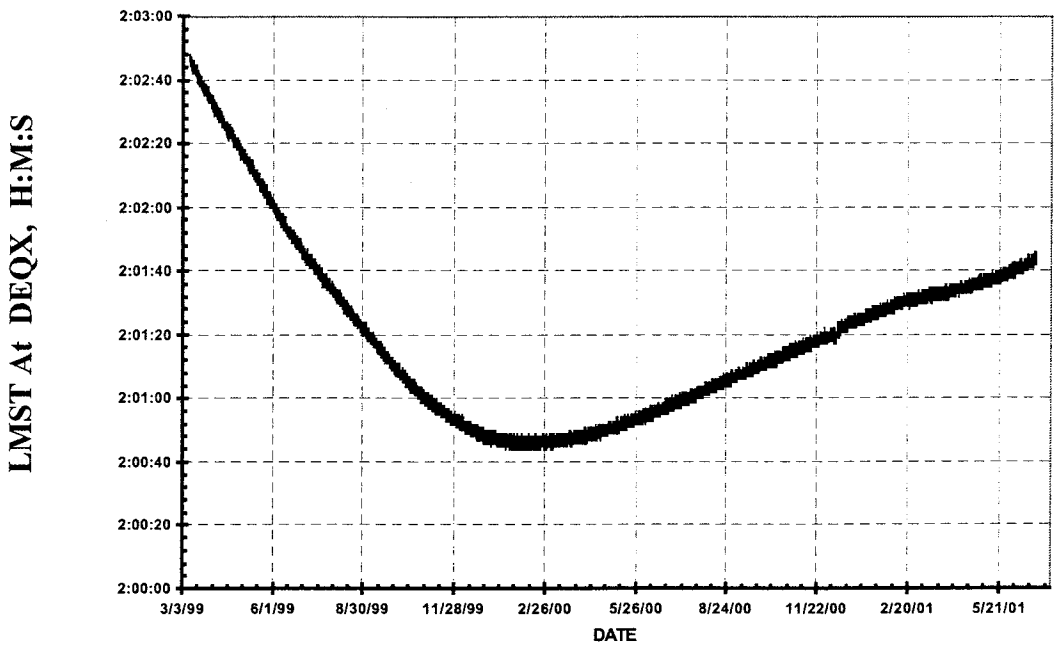

Figure 8 Orbit Local Mean Solar Time At The Descending Equator Crossing

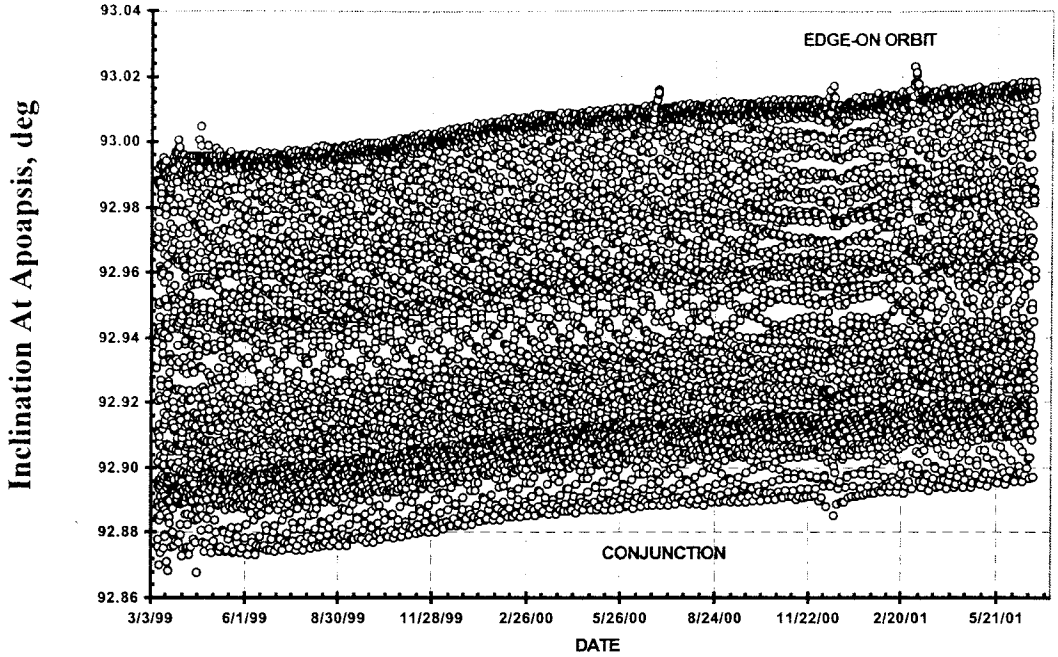

Figure 9 Orbit Inclination Variation (3/9/99 To 6/25/01)

ORBIT CONTROL

Prior to the MGS mission, the Mars Observer mission was to employ a concept of "strict longitude grid control" in order to achieve a uniform distribution of ground tracks. The objective was to specify, prior to the beginning of the mapping mission, a uniform distribution of ground tracks with 3 km spacings at the equator over a supercycle consisting of 6917 orbits over 550 sols. Thus propulsive maneuvers were planned, every two weeks, primarily to adjust the orbit period to achieve the ideal GTW; this was referred to as "flying to the grid". During planning for the MGS mission, the implementation of "strict longitude grid control" for the mapping orbit was abandoned. However, the concept of an ideal GTW at 58.6 km eastward was maintained but no longer as a requirement.

During the 695 days of the MGS mapping phase, only three OTMs were executed. These were for refinement of the frozen orbit parameters and GTW control. Characteristics of the maneuvers are given in Table 3. Note that the GTW target for OTM-1 was not achieved due to thruster plume impingement on the HGA during execution of the maneuver (see Figure 1). However, most of the frozen orbit targets were achieved (see Figs. 3 and 4). On two other occasions (August and December, 2000), OTM execution for GTW control was investigated but not implemented for a variety of reasons. Among these was the unexpected nature of the AMDs and thruster plume

impingement on the HGA. In effect, the AMDs were acting as mini-maneuvers and perturbing the semi-major axis in small but noticeable ways especially after solar conjunction.

Table 3

MGS ORBIT TRIM MANEUVERS (OTM)

Event/Parameter	OTM-1	OTM-2	OTM-3
Purpose	Adjust GTW/refine frozen orbit	Adjust GTW/refine frozen orbit	Adjust GTW
Date, ET	05/07/99	06/10/99	08/11/99
Mapping orbit	729	1144	1905
Delta-velocity, m/s	3.54	0.181	0.373
Delta-hydrazine,kg	-1.19	-0.059	-0.12
Burn duration, sec	93.5	5.3	11.1
True anomaly, deg	64.1	-84.0	-128.
Delta-GTW, km	29. (target)	25.	-22.
Delta-a, km	-0.45	-0.42	0.39
Delta-period, sec	-1.26	-1.17	1.09

ORBIT PERTURBATIONS

The primary orbital perturbation acting on the MGS orbit is due to frequent AMDs and the associated thruster plume impingement on the HGA. For MGS, attitude is maintained by a series of three RWAs each mounted along the spacecraft's X-Y-Z body axes. When angular momentum in a RWA reaches a threshold, nominally at 10 Nms, wheel desaturation occurs by activating a pair of thrusters. Ideally, any AMD event should not impart a translational perturbation along the spacecraft's X axis; note that the minus X-axis is close to the velocity direction of the spacecraft. During primary mapping, the frequency of spin axis AMDs was variable but on average occurred every 7.5 hours for a total of approximately 2200 events. Spin-axis AMDs refer to the Y-axis RWA which has its rotation axis along the spacecraft's +Yaxis and is aligned with the angular momentum vector of the orbit. Yaw axis AMDs occurred less frequently, on average every 30 hours yielding a total of approximately 550 events. Yaw-axis AMDs unload the Z-axis RWA; the spacecraft's +Z-axis is along the nadir direction. Spin axis AMDs generated larger orbital perturbations. During various intervals of the mapping phase, it became apparent that small AMD-induced, velocity perturbations were acting along the velocity direction of the spacecraft. This is evident in Figure 10 which shows a

dramatic and positive, period trend especially after solar conjunction. We attribute this perturbation to thruster plume impingement on the HGA and it's responsible for the strong negative trend in the GTW shown in Figure 1.

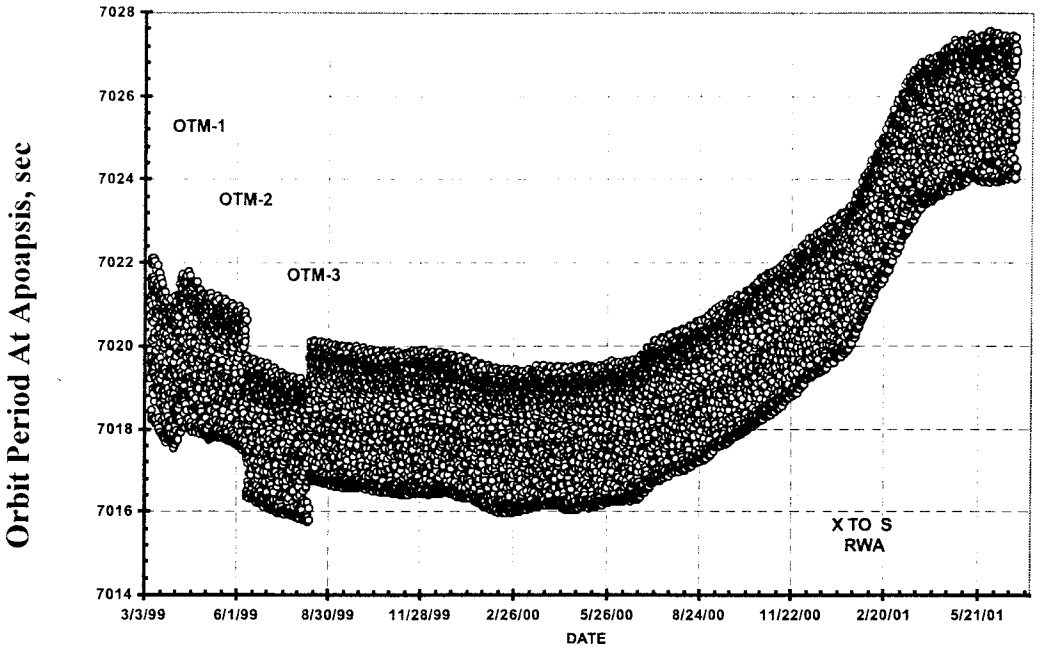

Figure 10 Variation In Osculating Orbit Period (3/9/99 To 6/25/01)

Orbital Influence of Angular Momentum Desaturations

In this section, we examine the individual effects of AMDs over several orbits especially on the semi-major axis and eccentricity which affect the GTW and frozen orbit. Primarily because of thruster plume impingement on the HGA during an AMD, the effective velocity perturbation is dependent on the HGA orientation during the desaturation. When AMDs occur, the thrusters are pulsing (0.09 sec on; 7.91 sec off) on average over a three minute interval which corresponds to 9.2 degrees change in true anomaly. In Figure 11 and the related Table 4, we show a small but representative effect of nine AMDs over a 72 hour span. Shown is the difference in osculating orbit elements, at apoapsis passage, between two trajectories. The first is the predicted trajectory which does not model any AMDs (for this case); the other is an accurate reconstruction of the same orbits in which all AMDs are individually estimated, as velocity perturbations, during the orbit determination process (Ref. 7). The definition of the orbit element

change or perturbation is, for example, a(reconstruct) = a(predict) + Δa. Thus, this figure shows the varying orbital perturbation due to each spin axis AMD during this interval. These perturbations are due to the integrated effect of the velocity perturbations. Effectively, these result from the x and z velocity components since the y component is close to zero. ΔV(z) varies mostly within 15-20 mm/sec per desaturation.

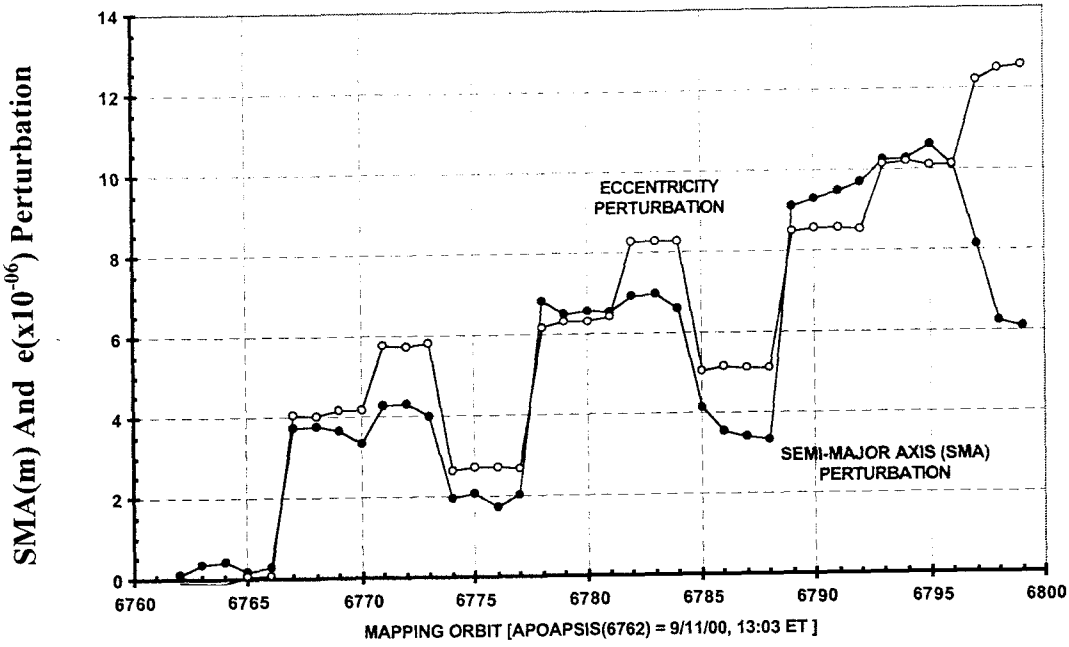

Figure 11 Orbital Perturbations Due To Nine AMDs

Table 4

MGS AMD-INDUCED ORBITAL PERTURBATIONS

AMD Epoch 9/11-14/00	True Anomaly deg	ΔV(x), mm/sec	Δa, m	Δe, (x10^{-06})
21:43:25	-41.9	-1.85	3.47	3.99
04:51:02	-165.9	0.03	0.96	1.60
12:16:51	130.5	0.48	-2.05	-3.16
19:17:33	-42.0	-1.84	4.80	3.48
02:25:58	-165.6	0.11	0.40	1.85
09:51:11	132.6	0.42	-2.48	-3.22
16:52:02	-40.9	-1.94	5.79	3.38
00:00:06	-165.6	0.15	0.53	1.61
07:50:52	-165.4	0.16	-1.98	2.07

Figure 12 is related to the previous figure and shows the orbital distribution and magnitude of the velocity perturbations due to 446 spin-axis AMDs during 9/1/00 to 1/17/01. Only the x-component of the velocity perturbation is shown; a negative $\Delta V(x)$ means the perturbation is close to the velocity direction of the spacecraft and tends to increase the semi-major axis or period as indicated in Figs. 10 and 11. There is a strong correlation between this perturbation at the –2 to –3 mm/sec level and the earth occultation interval when the HGA is in a fixed, parked position or orientation. The HGA is also in the parked position at two other times namely, during a "HGA rewind" as indicated in the figure and during non-tracking periods also called "non-communication" orbits. The small positive $\Delta V(x)$ values occur primarily during "communication orbits" when the HGA is tracking the earth. This type of analysis has helped us to: a) identify where along the orbit the AMD perturbation most influences the period and GTW and b) approximate the effect of future AMDs and thereby considerably improve the accuracy of our predictions.

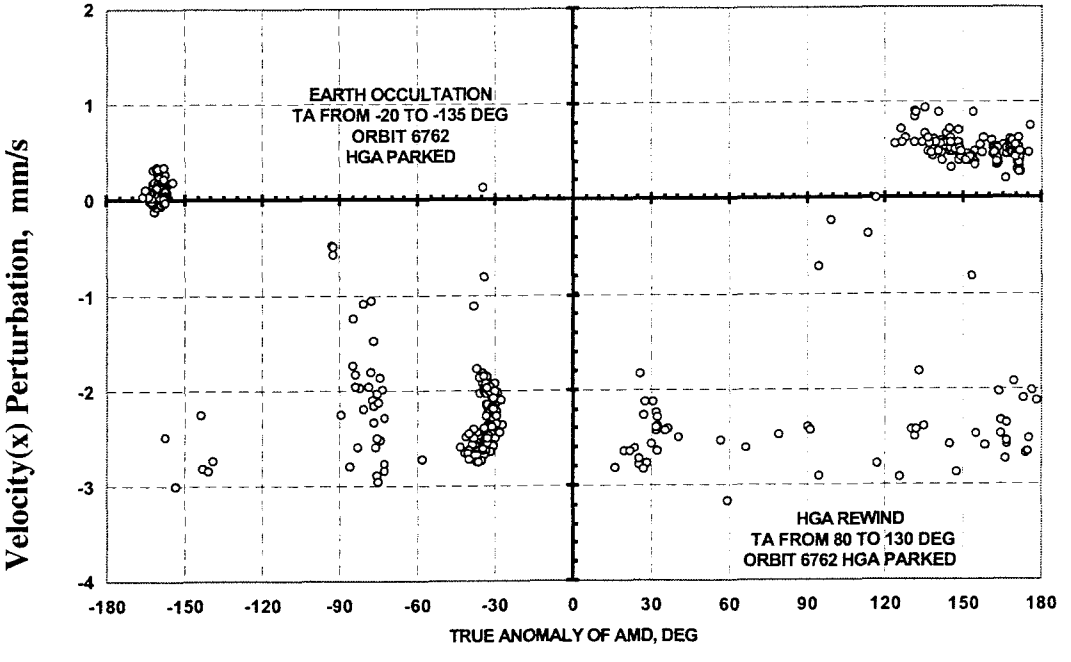

Figure 12 Distribution of Spin Axis AMDs And The Induced Velocity Perturbation (9/1/00 To 1/17/01)

Mars Gravity Field Models

Before the operational phase of the MGS mission, various Mars gravity field models resulting from the Mariner 9 and Vikings 1 and 2 missions were used to design a set of orbit elements defining the frozen mapping orbit. After MGS aerobraking and during the gravity calibration phase, both the Navigation and Radio Science Teams analyzed Doppler data and significantly improved existing Mars gravity field models. In particular, an interim navigation-developed model was used to establish the orbital targets for the transfer-to-mapping-orbit maneuver. This established the initial, frozen mapping orbit on 2/19/99. Thereafter, successively more accurate gravity models were developed by the Radio Science Team, usually of degree and order 75x75, which are being used to navigate MGS. These gravity field refinements were important for: a) planning and executing OTMs, b) analysis of the Doppler data to provide more accurate reconstruction of AMDs and thereby the spacecraft's state (Ref. 7), and c) the generation of predicted orbital evolution usually over 17 days but also as long as 180 days. The result of this effort is that the orbital perturbations due to the gravity field are well understood and thus a minor source of error.

PREDICTION CAPABILITY

In addition to evaluating and assessing the evolution of the MGS orbit in a reconstructed sense, we must also predict the orbit evolution. This is necessary a) for planning engineering activities and science observations and b) for insuring that the orbit remains within specific tolerances or bounds. Down track or equator crossing time predictions are the largest source of spacecraft positional error. Compilation of a post AMD history database coupled with an expectation of future AMD events and a real-time monitor of current navigation predictions provide the basis for estimating future AMD perturbations. A set of representative Tdeqx errors and their growth for eight separate orbit evolution predictions made during February 2001 are given in Figure 13. These errors were generated by differencing the predicted Tdeqx (per analysis) with the accurately reconstructed times determined from analysis of Doppler tracking data. Tdeqx errors are within 10 seconds over a prediction interval of 17 days (208 orbits) and less than 1.5 seconds over 5 days (61 orbits). The former interval is the project requirement for developing and implementing a series of commands transmitted to the spacecraft (called uplinking a sequence) during beta supplement. In particular, note that the predicted ephemeris generated on 2/20/01 was accurate to within 2 seconds throughout the entire 20 day interval shown. For this case, the influence of future AMDs was very accurately accounted for with this mean acceleration model, Ap = $(-1.0, 0.0, 8.0)\times10^{-10}$ km /sec^2. However, whenever unexpected events occur, as for example, the failure of the X RWA and the transition to the S RWA on 1/18/01 or the spacecraft's entry into

contingency mode on 5/2/01, the character or orbital effect of the AMDs will change. Thus, the accuracy of Tdeqx predictions made previous to this event will degrade. For example, the navigation timing prediction made on 1/16/01, just prior to the X-axis RWA failure, reached a large error of –50 seconds after 17 days of prediction.

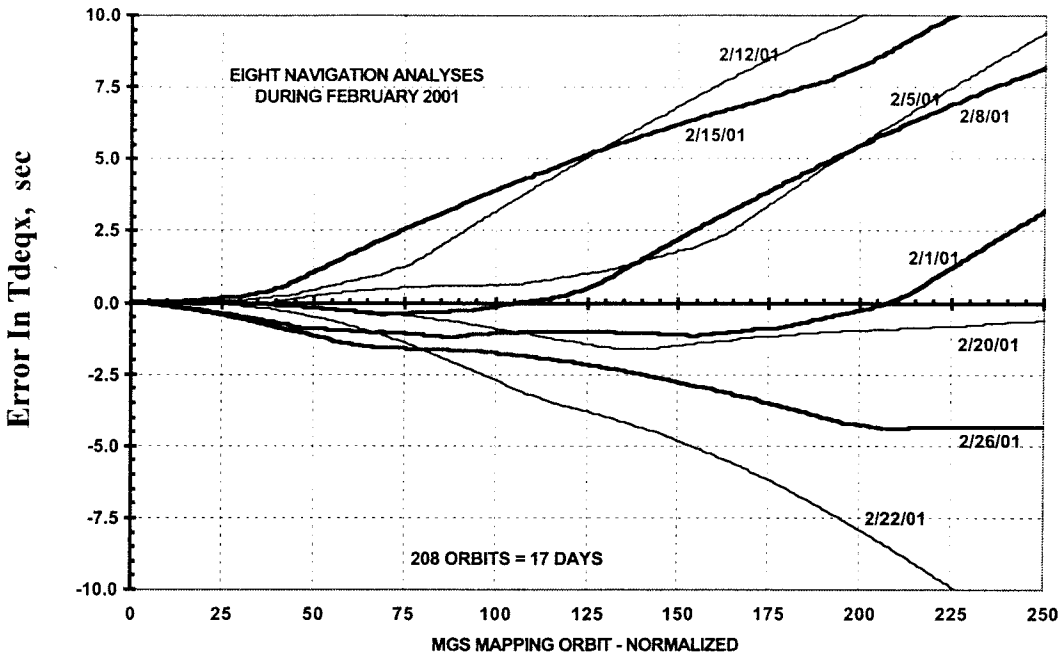

Figure 13 Error In Down Track Or Tdeqx Predictions For Eight Analyses Generated On The Dates Shown

A long term, predicted, down track (or Tdeqx) error assessment has been made over a 180 day interval. This was done for MGS science data acquisition planning and for preparing MGS as a relay satellite for the EDL phase of the MER mission. Synchronization of MGS over the MER descent to Mars will be necessary and shall be achieved with propulsive maneuvers starting several months earlier. The secular growth in down track errors, for five cases, is given in Table 5. After 180 days of prediction, timing errors are within the 25-50 minute range or about one-quarter to one-half of an orbit. The large initial error for the 1/12/01 ephemeris prediction is due to the X RWA failure on 1/18/01 and thus, the changed nature of the AMD-induced orbital perturbations. Our mean acceleration model used to account for future AMDs in this prediction was Ap = (-0.35, 0.0, 5.93) x 10^{-10} km/sec^2. After the RWA failure, a more accurate acceleration model was determined to be Ap = (-0.90, 0.0, 5.93) x 10^{-10} km/sec^2.

Table 5

LONG TERM Tdeqx ERROR (MIN) OVER 180 DAYS

Analysis Date	After 60 Days	After 120 Days	After 180 Days
09/15/00	-0.895	-6.11	-25.8
10/13/00	-1.85	-10.2	-40.8
11/10/00	-2.13	-16.2	-48.6
12/08/00	-1.94	-16.2	-50.3
01/12/01	-9.85	-33.9	-49.3

Our most recent six month, predicted ephemeris was generated on 6/29/01 after the end of the beta supplement phase. After several days in this new spacecraft operational mode, an updated AMD-induced, mean acceleration model was developed and applied throughout this prediction interval , Ap = (0.30, 0.0, 6.0) x 10^{-10} km/sec^2. The x component of the acceleration was aligned close to the anti-velocity direction of the spacecraft. The resultant orbit evolution predicts a mean decrease in the semi-major axis of 41.8 m per eighty-eight orbits or a period change of –0.12 sec per eighty-eight orbits. This, in turn results in a GTW slope of 2.46 km per eighty-eight orbits which projects to a GTW of –38 km by the end of 2001. After sixteen days into nominal flight operations (i.e. after the beta supplement mode), the reconstructed GTW variation exhibits a secular increase of 2.5 km per eighty-eight orbits.

CONCLUSIONS

The following conclusions are a result of navigating MGS throughout the primary mapping mission and several months into the extended mission: a) the mapping orbit evolution and control have successfully maintained the orbit within the requirements established for the primary mapping mission, b) the predicted orbital analyses have satisfied science objectives; this is especially true for very short-term predictions required for accurate image targeting, c) autonomous AMDs have had a strong influence on the GTW evolution and were especially noticeable after solar conjunction, d) thruster plume impingement was not identified during the development phase of the MGS mission but during flight operations was established as the primary perturbing influence on the GTW, e) an AMD database was established and correlated with orbital perturbations; this allowed navigation to develop perturbative acceleration models used effectively in prediction orbital evolution and f) changes in spacecraft operations, such as, MGS entering contingency mode, parking the HGA for long periods as occurred during solar conjunction and the failure of the X-axis RWA, have had a pronounced effect on the orbit period and consequently on the GTW.

ACKNOWLEDGEMENTS

The work described in this paper was conducted at the Jet Propulsion Laboratory, California Institute of Technology, under a contract with the National Aeronautics and Space Administration. The authors would like to acknowledge the contributions of the MGS project personnel, our LMA colleagues, especially Stuart Spath and Dave Eckart, the Radio Science Team, especially William Sjogren and Dah-Ning Yuan, and the DSN for radiometric data aquisition.

REFERENCES

1. C. Uphoff, "Orbit Selection for a Mars Geoscience/Climatology Orbiter," AIAA 22nd Aerospace Sciences Meeting, AIAA-84-0318, Reno, NV, January 9-12, 1984.

2 A. Albee et al, "Overview of the Mars Global Surveyor Mission," JGR-Planets, publication date September, 2001.

3. P. B. Esposito, V. Alwar, P. Burkhart, S. Demcak, E. Graat, M. Johnston, and B. Portock, "Navigating Mars Global Surveyor through the Martian Atmosphere: Aerobraking 2," AAS/AIAA Astrodynamics Specialist Conference, AAS-99-443, Girdwood, AK, August 16-19, 1999.

4. Joseph Neelon, Stuart Spath, and Wayne Sidney, "Mars Global Surveyor Azimuth Gimbal Anomaly: The Analysis Of The Problem And Solution, And The Implementation", paper AAS 00-198, AAS/AIAA Space Flight Mechanics Meeting, Clearwater, Florida, January 23-26, 2000.

5. W. D. McClain, "Eccentricity Control and the Frozen Orbit Concept for the Navy Remote Ocean Sensing System (NROSS) Mission", Paper AAS 87-516, AAS/AIAA Astrodynamics Specialist Conference, Kalispell, Montana, 8/10-13/87.

6. P. Esposito et al, "Mars Global Surveyor: Navigation and Aerobraking at Mars," Proceedings of the 13th International Symposium on Space Flight Dynamics, Goddard Space Flight Center, Greenbelt, Md, May 11-15,1998, Spaceflight Dynamics 1998, editor Thomas H. Stengle, Volume 100, Part II, Advances in the Astronautical Sciences, Published for the American Astronautical Society by Univelt, Inc, San Diego, CA 92198.

7. Stuart Demcak, Pasquale B. Esposito, Darren T. Baird, Eric Graat, "Mars Global Surveyor Mapping Orbit Determination", AAS/AIAA Space Flight Mechanics Meeting, AAS-01-100, Santa Barbara, CA, February 11-15, 2001.